Am J Transl Res 2016;8(6):2549-2561
www.ajtr.org /ISSN:1943-8141/AJTR0025570

Original Article

Periprostatic implantation of neural differentiated mesenchymal stem cells restores cavernous nerve injury-mediated erectile dysfunction

Jia-Feng Fang[1*], Chang-Chang Jia[2*], Zong-Heng Zheng[1], Xiao-Long Ye[1], Bo Wei[1], Li-Jun Huang[1], Hong-Bo Wei[1]

[1]*Department of Gastrointestinal Surgery, The Third Affiliated Hospital of Sun Yat-sen University, Tianhe Road 600, Guangzhou 510630, China;* [2]*Cell-Gene Therapy Translational Medicine Research Center, The Third Affiliated Hospital of Sun Yat-sen University, Tianhe Road 600, Guangzhou 510630, China.* [*]*Equal contributors.*

Received February 4, 2016; Accepted May 3, 2016; Epub June 15, 2016; Published June 30, 2016

Abstract: Mesenchymal stem cells (MSCs) have been utilized to restore erectile function in animal models of cavernous nerve injury (CNI). However, transplantation of primary MSCs may lead to unpredictable therapeutic outcomes. In this study, we investigated the efficiency of neural differentiated MSCs (d-MSCs) on the restoration of erectile function in CNI rats. Rat bone marrow MSCs (r-BM-MSCs) were treated with all-trans retinoic acid to induce neural differentiation. Rats were divided into five groups: a sham operation group; a bilateral CNI group that received an intracavernous injection of r-BM-MSCs (IC group); and three groups that received periprostatic implantation of either r-BM-MSCs (IP group), d-MSCs (IP-d group), or PBS (PBS group). The data revealed that IP injection of d-MSCs ameliorated erectile function in a similar manner to an IC injection of MSCs and enhanced erectile function compared to an IP injection of MSCs. An *in vivo* time course of d-MSCs survival revealed that PKH26-labled d-MSCs were detectable either within or surrounding the cavernous nerve tissue. In addition, the expression of caspase-3 significantly increased in the PBS group and decreased after treatment with MSCs, especially in the IC and IP-d groups. Furthermore, the expression levels of neurotrophic factors increased significantly in d-MSCs. This study demonstrated that periprostatic implantation of d-MSCs effectively restored erectile function in CNI rats. The mechanism might be ascribed to decreases in the frequency of apoptotic cells, as well as paracrine signaling by factors derived from d-MSCs.

Keywords: Mesenchymal stem cell, erectile dysfunction, cavernous nerve injury, nerve differentiation, stem cell therapy

Introduction

Postoperative erectile dysfunction (ED) resulting from damage of pelvic autonomic nerve (PAN) is a frequent complication of pelvic surgery [1-3]. Pelvic autonomic nerve preservation is widely performed to maintain urogenital function [4-8]. However, PAN damage cannot be completely prevented, and damage to this nerve results in a high incidence of ED, suggesting that additional methods should be developed to repair the PAN and restore sexual function.

Mesenchymal stem cells (MSCs) have the potential to undergo multi-lineage differentiation and are also able to replace necrotic or apoptotic cells [9, 10]. Recently, based on mouse and rat models of cavernous nerve injury (CNI) induced ED, intracavernous and periprostatic implantations of MSCs were both able to restore erectile function [11, 12]. However, direct transplantation of MSCs may lead to unpredictable therapeutic outcomes due to the multi-lineage differentiation potential of this cell type [13, 14]. Therefore, we hypothesized that neural differentiation of MSCs might help to resolve this problem.

All-trans retinoic acid (ATRA), an active form of vitamin A, is an effective inducer of neural cell differentiation [15]. Previous studies have

revealed that pre-activation of ATRA facilitated neural differentiation of MSCs [16] and that transplantation of ATRA-induced MSCs promoted functional recovery of learning and memory in a rat model of hypoxic-ischemic brain damage [17]. Therefore, in the present study, we used ATRA to induce neural differentiation of MSCs (d-MSCs), and investigated the ability of d-MSCs to treat ED in a rat model of CNI.

Materials and methods

Ethics

This study was approved by the Institutional Animal Care and Use Subcommittee of the Third Affiliated Hospital of Sun Yat-sen University (201210016). All experiments were performed in accordance with their approved guidelines.

Isolation and culture of rat bone marrow MSCs (r-BM-MSCs)

Institutional Review Board approval was obtained for all procedures. Rat bone marrow MSCs were isolated from 4-week-old Sprague-Dawley rat femurs as previous described [18]. The cells were cultured in Dulbecco's Modified Eagle's Medium (DMEM) supplemented with 10% fetal bovine serum (FBS) and glucose (4.5 g/l) at 37°C in 5% CO_2. All non-adherent cells were removed and the medium was changed every 3 days.

Characterization of r-BM-MSCs

R-BM-MSCs were incubated with fluorescein isothiocyanate-conjugated antibodies for 30 minutes at 4°C. The following antibodies were used for flow cytometric analysis: CD14, CD34, CD45, CD73, CD90 and CD105. Cells were washed twice with PBS containing 0.1% bovine serum albumin. A FACScan machine (Becton, Dickinson, Franklin Lakes, NJ, USA) was used to analyze antibody binding.

Cells at passage 2 were used to assess the *in vitro* differentiation potential of MSCs into adipocytes and osteocytes as described previously [11]. Cells were cultured in the following medium types: (1) adipogenic differentiation medium (DMEM with 1 g/ml glucose, DMEM-LG) containing 10% FBS, 50 μg/ml of ascorbate-1 phosphate, 0.1 μmol/L dexamethasone and 50 μg/ml indomethacin; (2) osteogenic differentiation medium (DMEM-LG containing 10% FBS, 50 μg/ml ascorbate-2 phosphate, 10^{-2} μmol/L dexamethasone, and 10 mmol/L β-glycerophosphate). The medium was changed every 3 days.

Neural differentiation of r-BM-MSCs

R-BM-MSCs were cultured in 60-mm culture dishes or 48-well culture plates, and incubated with DMEM for 24 h. The medium was then changed to DMEM containing 1.0 μmol/L ATRA (Sigma, 10 mmol/L storage concentration in 100% ethanol), and cells were maintained for 48 h. Cells were then washed twice with D-Hank's and cultured in neural induction medium (NIM) containing DMEM, 1.6% dimethyl sulfoxide, 160 μmol/L butylated hydroxyanisole, 20 mmol/L KCl, 1.6 mmol/L valproic acid, 8 μmol/L forskolin, 0.8 μmol/L hydrocortisone and 4 μg/mL insulin (all from Sigma) for 48 h.

Immunofluorescent staining of induced cells

Neural induced cells were fixed with methanol at -20°C for 15 min and washed twice with PBS. Then, the fixed cells were blocked with 3% BSA and 0.1% Triton-X 100, followed by incubation with an anti-nestin antibody at 4°C overnight. After washing twice with PBS, cells were incubated with DyLight 546-conjugated secondary antibodies (Jackson ImmunoResearch) for 1 h and washed twice with PBS. Nuclei were stained with 4',6-diamidino-2-phenylindole dihydrochloride (DAPI) (Sigma). The cells were examined under a fluorescence microscope (TE2000-S; Nikon). Cells stained with isotype control primary antibodies were used as negative controls.

PKH26 labeling

To determine the *in vivo* engraftment of MSCs into the tissues of CNI rats, the cells were stained with PKH26 dye (catalogue.# mini26, Sigma Chemical Co.) according to the manufacturer's protocol. Depending on the site into which MSCs were injected, PKH26-labled MSCs were detected in either the corpus cavernosum or the cavernous nerve 2, 4 and 7 days after implantation (2 rats per group per time point).

Animal treatment

Eight-week-old male Sprague-Dawley rats (mean weight, 250 g) were obtained from the

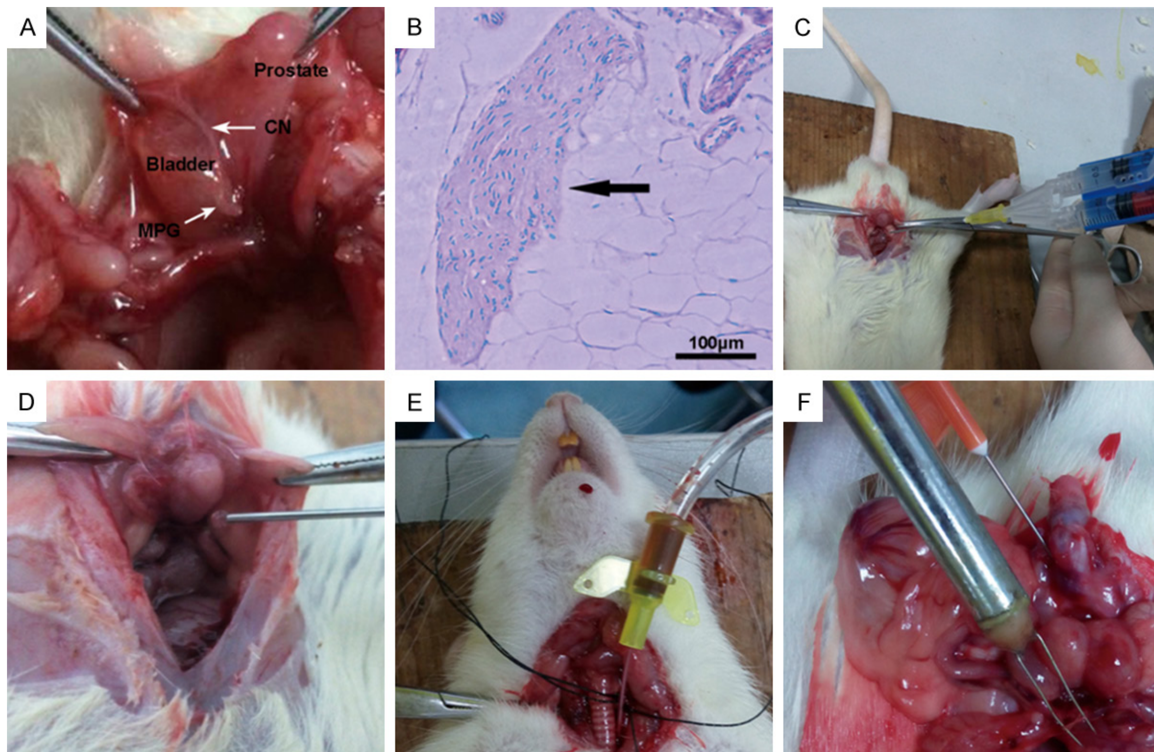

Figure 1. Animal treatment and evaluation of erectile function. A. Exposure of the major pelvic ganglias (MPGs) and the cavernous nerve (CNs). B. Pathological examination confirms the identity of CN tissue. Scale bar = 100 μm. C. In both the IP and IP-d groups, fibrin scaffolds of cells in PBS are prepared using a Porcine Fibrin Sealant Kit. D. The mixtures of cells and fibrin scaffolds are injected around the prostate. E. A heparinized 24-gauge silastic cannula is inserted to measure mean arterial pressure (MAP). F. The CN is exposed and stimulated with a bipolar electrode. Meanwhile, a heparinized 23-gauge butterfly needle is inserted into the corpus cavernosum to measure the intracavernous pressure (ICP).

Guangdong Medical Laboratory Animal Center and housed in a standard animal facility with 12-hlight/dark cycles. All animals were acclimatized for at least one week prior to surgery and allowed *ad libitum* access to standard food and water. All surgical procedures were performed by the same investigator, and all subsequent analyses were performed by another investigator. A pilot study was conducted to enhance the investigator's surgical skills, and to ensure that no animals experienced accidental death or required a humane sacrifice prior to the end of the study.

To ensure that sufficient samples were available for analysis, 10 rats per group were utilized. Each rat was intraperitoneally anesthetized with chloral hydrate (0.35 ml/100 g). A 3-4 cm lower abdominal midline incision was used to identify and expose the bilateral major pelvic ganglias (MPGs) and the CNs (**Figure 1A**, **1B**). Bilateral CNI was induced in 40 rats (CNI group) and another 10 rats underwent laparotomy (sham group) at random. In the CNI group, bilateral CNs were crushed with a non-serrated hemostat (Karl Stortz Co., Tuttlingen, Germany), with full tip closure 1 mm distal to the MPG for 2 minutes. Then, the CNI group was randomly divided into four groups of 10 rats each, which received (1) an intracavernous injection of r-BM-MSCs ($1×10^6$ cells in 20 μL of PBS) (IC group); (2) periprostatic implantation of r-BM-MSCs ($1×10^6$ cells in 20 μL of PBS) (IP group); (3) periprostatic implantation of d-MSCs ($1×10^6$ cells in 20 μL of PBS) (IP-d group); or (4) periprostatic implantation of 20 μL PBS (PBS group).

All cell injections and implantations were performed as previously described [11, 12] (**Figure 1C**, **1D**). In the IP and IP-d groups, fibrin scaffolds of cells in PBS were prepared using a Porcine Fibrin Sealant Kit (Hangzhou Puji Medical Technology Development Co. Ltd,

China) according to the manufacturer's instructions. The mixtures of cells and fibrin scaffolds were implanted around the prostate and into the MPG. In the IC group, 20 μL of cells in PBS were injected into the corpus cavernous using a 30-gauge needle. Before injection, drainage of the dorsal vein was blocked by circumferential compression of the base of the penis using an elastic band. The compression was released one minute after injection.

Evaluation of erectile function

Erectile function was evaluated by electrical stimulation of the CN as previously described [19], using a BL-420s Biological Functional System (Chengdu Taimeng Technology Ltd, China). Two weeks after cells injection, the rats were intraperitoneally anesthetized with chloral hydrate (0.35 ml/100 g). A midline incision from the neck to the upper thorax was made to expose the right carotid artery. Then, a heparinized 24-gauge silastic cannula was inserted to measure mean arterial pressure (MAP) (**Figure 1E**). The skin of the penis was then stripped off to expose the corpus cavernosum and a heparinized 23-gauge butterfly needle was inserted into the penile crus and connected to polyethylene-50 tubing to measure the intracavernous pressure (ICP). The CN was then exposed and stimulated with a bipolar electrode (5 V at 12 Hz for 60 seconds). During tumescence, the maximal ICP (mICP) and total ICP (tICP, area under the curve) were recorded (**Figure 1F**). The ratios of mICP and tICP to MAP were calculated to evaluate erectile function.

Immunofluorescence and immunohistochemical staining

Penile segments were harvested, cut into 10-μm thick frozen tissue sections and stored at -80°C. For fluorescence microscopy, penile sections were fixed in methanol for 10 minutes at 4°C, washed three times with PBS and blocked with 3% BSA and 0.1% Triton-X 100 for 1 h at room temperature. The tissue sections were incubated with primary antibodies to PECAM-1 (platelet/endothelial cell adhesion molecule, an endothelial cell marker, catalogue.# A2104, ABclonal Biotech Co., Ltd, USA; 1:100), α-actin (a smooth muscle cell marker, catalogue.# SC-130616, Santa Cruz Biotechnology, Santa Cruz, CA, USA; 1:100), and nNOS (neuronal nitric oxide synthase; catalogue.# A1485, ABclonal Biotech Co., Ltd, USA; 1:100) at 4°C overnight. Control sections were incubated without primary antibodies. After washing thrice with PBS, sections were incubated with DyLight 488 or 556-conjugated secondary antibodies (Invitrogen) for 1 h and washed thrice with PBS. Nuclei were stained with DAPI. Signals were visualized and digital images were obtained with a fluorescence microscope.

For immunohistochemical staining, tissue sections were fixed in cold methanol and blocked with 3% BSA and 0.1% Triton-X 100 for 1 h at room temperature. Then, the slides were stained with primary antibodies against caspase-3 (catalogue.# 9662, Cell Signaling Technology Co., Ltd, USA; 1:400). Immunoreactions were detected with the Dako-Cytomation Envision HRP System (Dako, Glostrup, Denmark), and the sections were counterstained with hematoxylin (Sigma, St. Louis, MO, USA). Negative controls were only stained with secondary antibodies.

Western blot

Equal amounts of protein (50 μg per lane) were electrophoresed on 8% sodium dodecyl sulfate polyacrylamide gels, transferred to nitrocellulose membranes, and probed with antibodies against caspase-3 (catalogue.# 9662, Cell Signaling Technology Co., Ltd, USA; 1:1000) or β-actin (catalogue.# 3700, Cell Signaling Technology Co., Ltd, USA; 1:1000). The results were quantified by densitometry (n = 4 per group).

Real-time PCR

Total RNA was extracted from MSCs using TRIzol reagent kit (Invitrogen, Carlsbad, CA). RNA was reverse transcribed using PrimeScript® RT reagent Kit (TaKaRa, Tokyo, Japan). Real-time PCR was performed on an ABI PRISM 7000 sequence detector (Applied Biosystems, Foster City, CA, USA) using SYBR® Premix Ex Taq™ (Perfect Real Time) (TaKaRa, Tokyo, Japan). GAPDH was used as an internal control. The primers used for the analysis are as follows: nestin, 5'-CTGAGGCCTCTCTTCTTCCA-3' (forward) and 5'-ACTCCTGTACCGGGTCTCCT-3' (reverse); vascular endothelial growth factor (VEGF), 5'-CGGGCCTCTGAAACCATGAA-3' (forward) and 5'-GCTTTCTG CTCCCCTTCTGT-

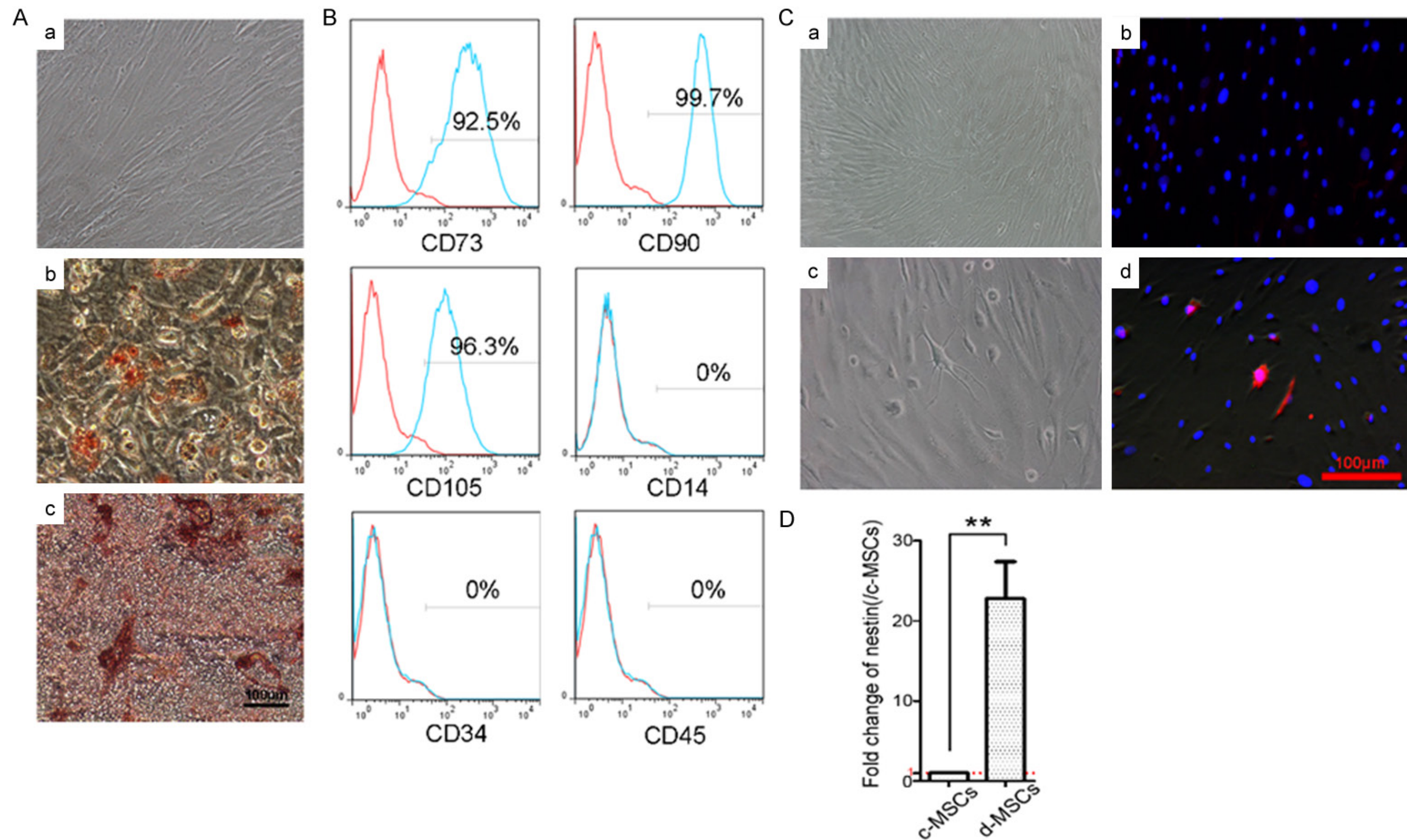

Figure 2. Isolation, characterization and neuronal differentiation of r-BM-MSCs. A. The morphology of r-BM-MSCs (a). After induction, the cells possessed the typical phenotypes of adipocytes (stained with oil red O) or (b) osteocytes (stained with alizarin red S) (c). Scale bar = 100 μm. B. Differentiated cells express the MSCs markers, CD73, CD90 and CD105, but do not express the hematopoietic or endothelial markers, CD14, CD34 and CD45. C. Neural differentiation of r-BM-MSCs. Control r-BM-MSCs (a). After induction with ATRA and culture in neural induction medium, r-BM-MSCs differentiate into neural-like cells, which exhibit large cell body diameters, long axons and dendrites (c). The neural stem cell marker, nestin, is expressed in the induced cells. Control MSCs express low levels of nestin (b), while induced-MSCs exhibit increased nestin expression (d). Scale bar = 100 μm. D. Assessment of expression level of nestin by real-time PCR. d-MSCs exhibited higher expression level of nestin than c-MSCs (control MSCs). $^{**}P < 0.01$.

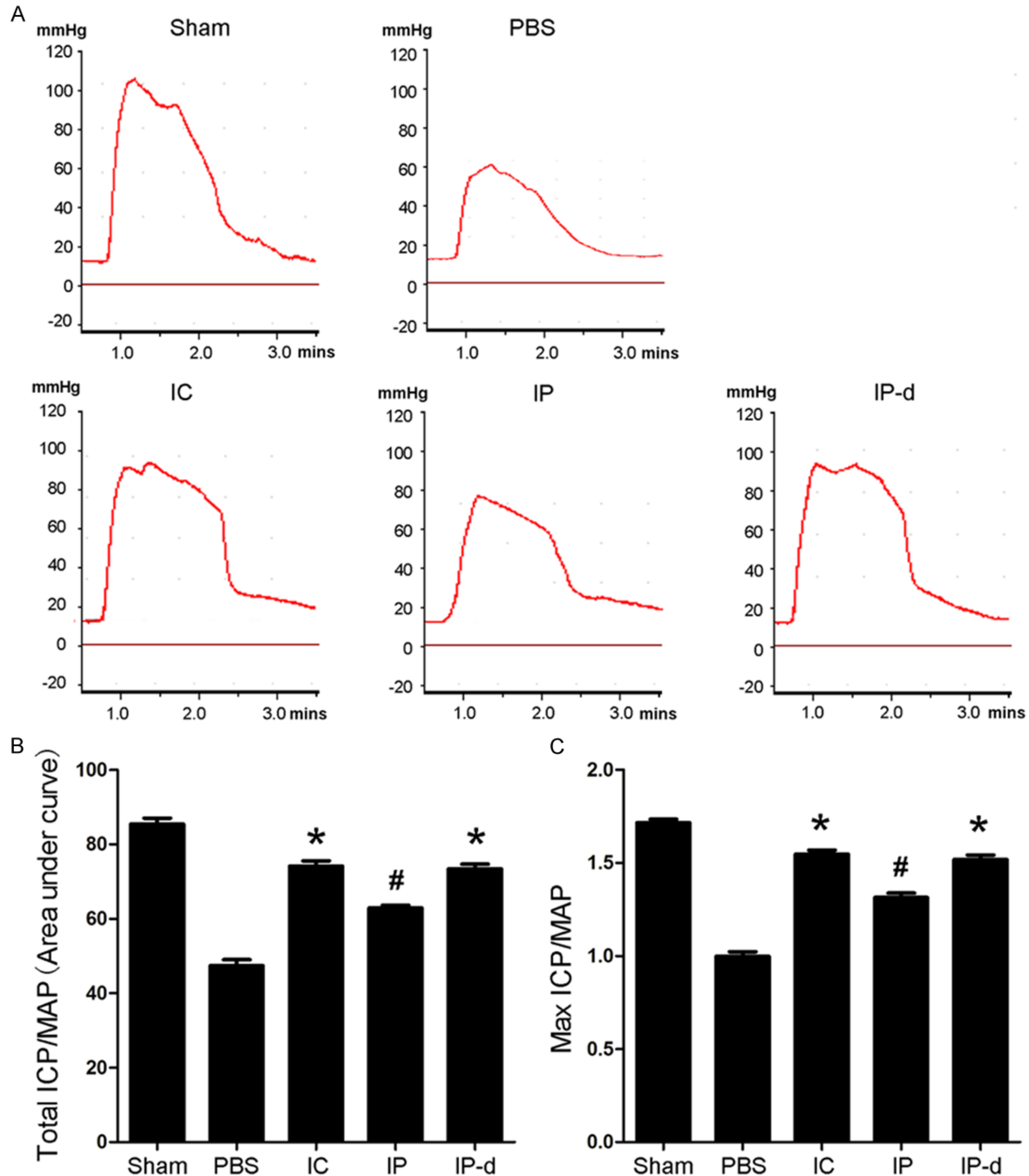

Figure 3. Effects of MSCs treatment on erectile function in animal models of bilateral CNI. A. Representative ICP responses for the sham group, CNI rats stimulated two weeks after intracavernous injection of r-BM-MSCs (1×10^6 cells/20 μL, IC group), and rats undergoing periprostatic implantation of r-BM-MSCs (1×10^6 cells/20 μL, IP group), d-MSCs (1×10^6 cells/20 μL, IP-d group), or 20 μL PBS (PBS group). B, C. The ratios of total ICP (area under the curve) and maximal ICP to MAP are recorded. Each bar depicts the mean ± standard deviation from n = 4 animals per group. $^*P < 0.01$ vs. PBS group, $^\#P < 0.05$ vs. IC, IP-d and PBS groups, respectively.

3' (reverse); nerve growth factor (NGF), 5'-ATAAGACCACAGCCACGGAC-3' (forward) and 5'-ACGCCTTGACAAAGGTGTGA-3' (reverse); brain-derived neurotrophic factor (BDNF), 5'-ATAAGACCACAGCCACGGAC-3' (forward) and 5'-ACGCCTTGACAAAGGTGTGA-3' (reverse); and GAPDH, 5'-GTTACCAGGGCTGCCTTCTC-3' (forward) and 5'-GATGGTGATGGGTTTCCCGT-3' (reverse).

Statistical analysis

Results were expressed as the mean ± standard deviations. Group comparisons of parametric data were evaluated by one-way analysis of variance (ANOVA) followed by Newman-Keuls post hoc analysis, while Kruskal-Wallis test was applied for analysis of nonparametric data. Statistical analyses were performed with SPSS (version 15.0, Chicago, IL, USA). All statistical tests were 2-sided, and $P < 0.05$ was considered significant.

Results

Isolation and characterization of r-BM-MSCs

Primary r-BM-MSCs were isolated from the femurs of 4-week-old Sprague-Dawley rats and cultured *in vitro*. MSCs in this study showed typical spindle, fibroblast-like morphology and were arrayed like whirlpools (**Figure 2Aa**). Cells at passage 2 were used to assess the *in vitro* differentiation potentials of MSCs into adipocytes and osteocytes. Differentiated cells possessed the typical phenotypes of adipocytes (stained with oil red O) and osteocytes (stained with alizarin red S) (**Figure 2Ab**, **2Ac**). In addition, as shown in **Figure 2B**, the cells expressed markers of MSCs, including CD73, CD90 and CD105, but did not express the hematopoietic or endothelial markers, such as CD14, CD34 and CD45.

Neural differentiation of r-BM-MSCs

After induction by ATRA and cultured in NIM, r-BM-MSCs differentiated into neural-like cells, which exhibited large cell body diameters, long axons, and dendrites (**Figure 2Cc**). To further characterize neural differentiation, expression of the neural stem cell marker nestin, was detected in the induced cells. The results revealed that d-MSCs expressed significantly higher levels of nestin compared to control MSCs (**Figure 2Cd**). In addition, the expression levels of nestin in both control MSCs and d-MSCs were assessed by real-time PCR. The results revealed that d-MSCs exhibited higher expression level of nestin than control MSCs (**Figure 2D**).

Effects of MSCs implantation on erectile function in bilateral CNI models

Erectile function was evaluated by electrical stimulation of the CN two weeks after treatment with MSCs or PBS. There were no significant differences in the MAP and basal ICP among the five experimental groups (data not shown). During tumescence, the maximal ICP (mICP) and total ICP (tICP, area under the curve) were recorded. As shown in **Figure 3**, the ratios of tICP/MAP and mICP/MAP decreased in the PBS group compared with those of the sham group, respectively (47.4±1.6 vs. 85.4±1.6, P < 0.01; 1.00±0.03 vs. 1.72±0.02, $P < 0.01$). After treatment with MSCs, the ratios of tICP/MAP and mICP/MAP increased significantly. The ratios of tICP/MAP and mICP/MAP in the IP-d group (73.4±1.21; 1.52±0.02) were similar with those in the IC group (74.1±1.5; 1.55±0.02), while better than the IP ones (62.9±0.73; 1.31±0.02, $P < 0.05$).

Endothelial and smooth muscle contents of the corpus cavernosum

After evaluation of erectile function, the rats were sacrificed, and penile segments were harvested and cut into frozen tissue sections for immunofluorescent or immunohistochemical staining. The tissue sections were incubated with antibodies to the endothelial cell marker, PECAM-1, or the smooth muscle cell marker, α-actin. The expression of PECAM-1 significantly decreased in the PBS group compared to the sham group, and markedly increased after treatment with MSCs (**Figure 4A**). Similarly, the expression of α-actin significantly decreased in the PBS group compared with the sham group, and increased after treatment with MSCs (**Figure 4B**). Moreover, the ratios of smooth muscle area to cavernous area in the IC and IP-d groups were higher than those in the IP ($P < 0.05$) and PBS groups ($P < 0.01$) (**Figure 4C**).

Expression of nNOS in the corpus cavernosum

The expression of nNOS in the corpus cavernosum was detected by immunofluorescent staining 2 weeks after injection with MSCs. The data revealed that nNOS expression significantly decreased in the PBS group compared to the sham group. Expression of nNOS increased in the IC, IP and IP-d groups the, yet was higher in both the IC and IP-d groups compared to the IP group (**Figure 5**).

In vivo time course of MSCs survival in CNI rats

To evaluate the *in vivo* survival of implanted MSCs over time, the cells were stained with

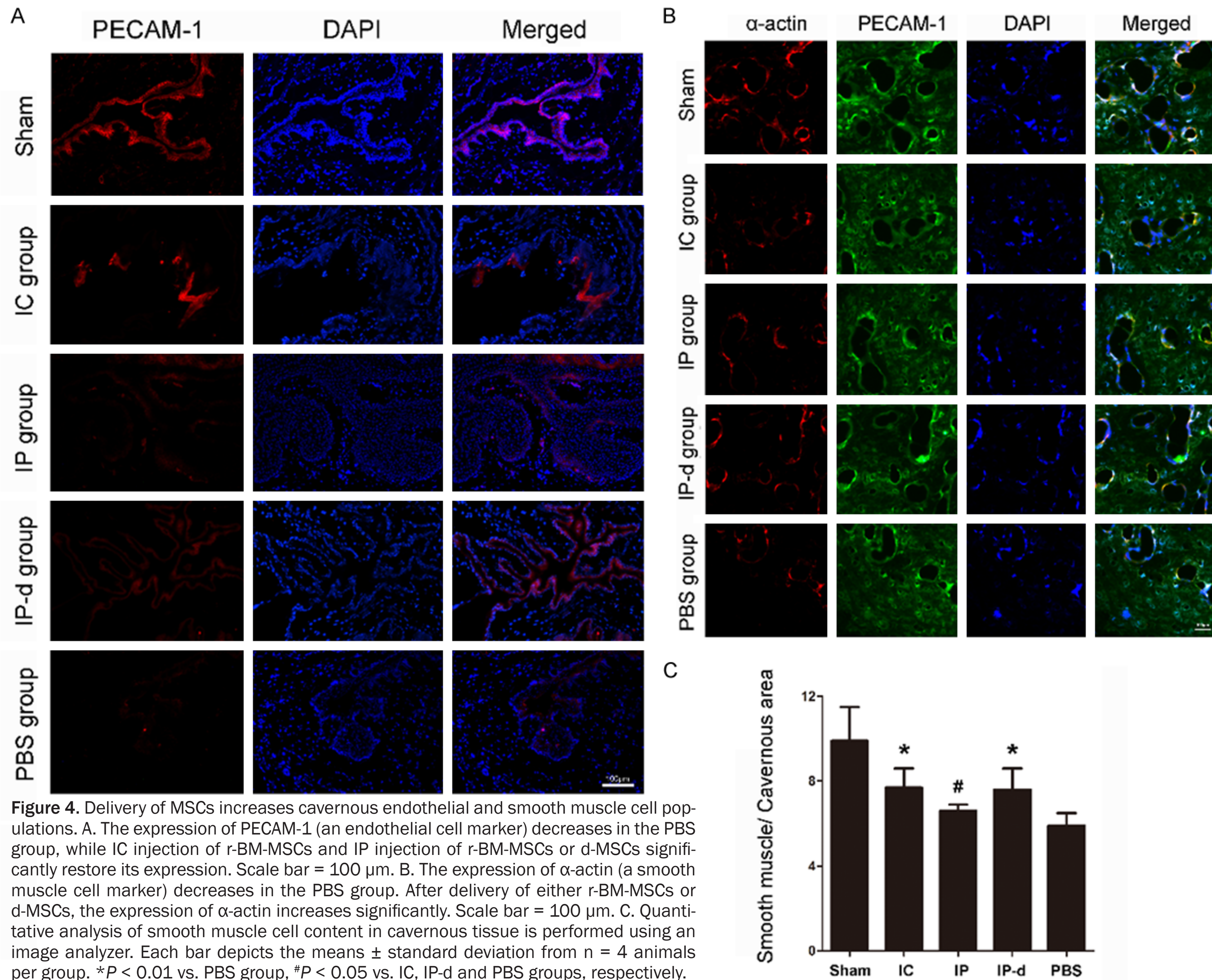

Figure 4. Delivery of MSCs increases cavernous endothelial and smooth muscle cell populations. A. The expression of PECAM-1 (an endothelial cell marker) decreases in the PBS group, while IC injection of r-BM-MSCs and IP injection of r-BM-MSCs or d-MSCs significantly restore its expression. Scale bar = 100 μm. B. The expression of α-actin (a smooth muscle cell marker) decreases in the PBS group. After delivery of either r-BM-MSCs or d-MSCs, the expression of α-actin increases significantly. Scale bar = 100 μm. C. Quantitative analysis of smooth muscle cell content in cavernous tissue is performed using an image analyzer. Each bar depicts the means ± standard deviation from n = 4 animals per group. **P* < 0.01 vs. PBS group, #*P* < 0.05 vs. IC, IP-d and PBS groups, respectively.

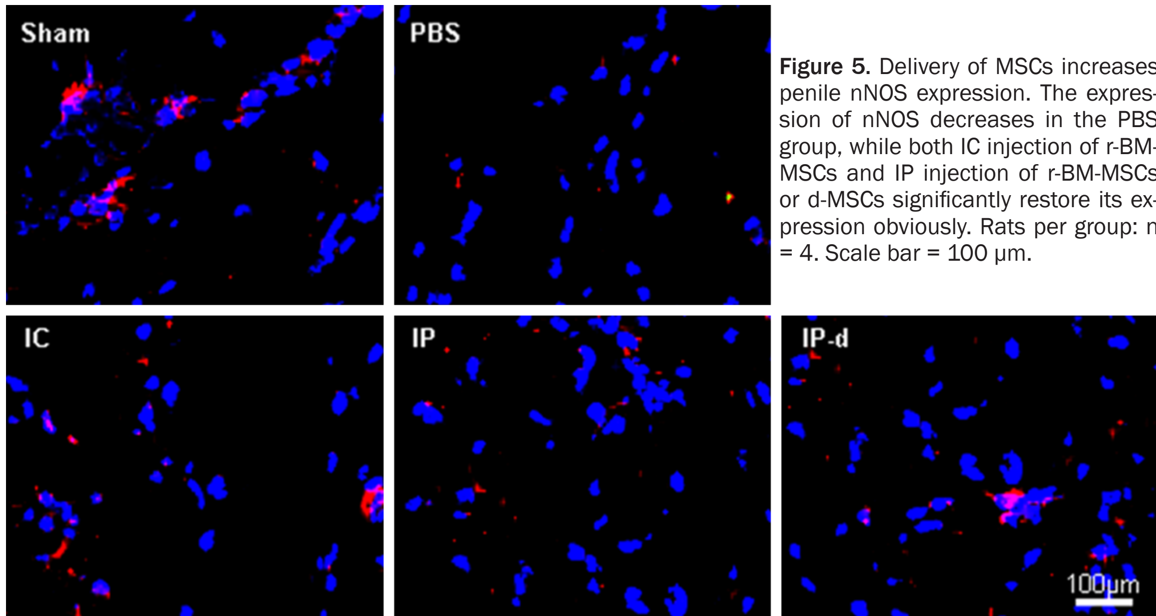

Figure 5. Delivery of MSCs increases penile nNOS expression. The expression of nNOS decreases in the PBS group, while both IC injection of r-BM-MSCs and IP injection of r-BM-MSCs or d-MSCs significantly restore its expression obviously. Rats per group: n = 4. Scale bar = 100 μm.

PKH26 dye. Depending on the site into which MSCs were injected, PKH26 labled MSCs were detected in either the corpus cavernosum or the CN 2, 4 and 7 days after implantation.

In the IC group, PKH26 labled MSCs were detectable in the corpus cavernosum. By contrast, in both the IP and IP-d group, PKH26 labled MSCs were detectable within and/or surrounding the CN, but not in the corpus cavernosum. However, PKH26 labled MSCs were detectable within the first 2 days after injection in the IP group, whereas they were not detectable until 7 days after treatment in the IP-d group (**Figure 6**).

Underlying mechanisms of MSCs-mediated restoration of erectile function

Both immunohistochemical staining and Western blot were performed to evaluate the expression of caspase-3 two weeks after injection with MSCs. The expression of either caspase-3 or cleaved caspase-3 significantly increased in the PBS group compared to the sham group, and decreased after treatment with MSCs, especially in the IC and IP-d groups (**Figure 7A**, **7B**).

In addition, the expression levels of VEGF, NGF, and BDNF in the different groups of MSCs were assessed by real-time PCR. As shown in **Figure 7B**, after induction with ATRA and culture in NIM, d-MSCs exhibited higher expression levels of VEGF, NGF, and BDNF than r-BM-MSCs in the group of control, single induced by ATRA or single cultured in NIM.

Discussion

Pelvic autonomic nerve preservation (PANP) is currently widely performed to maintain urogenital function during pelvic surgery [4-7]. However, damage to the PAN cannot be completely prevented, and damage to this nerve responsible for approximately 45% of ED cases. Phosphodiesterase type 5 inhibitors are successfully used to treat ED [20]. However, these drugs are not satisfactory for treating patients with PAN damage. Thus, new strategies to treat nerve damage-induced ED are urgently needed.

MSCs have been shown to exhibit multi-lineage differentiation potentials and can replace necrotic or apoptotic cells [9, 10]. Previous studies have revealed that delivery of MSCs was effective for treating ED in animal models of aging, diabetes and nerve-injury [11, 12, 21-23]. In the present study, we showed that both intracavernous and periprostatic implantations of MSCs were effective treatment strategies for nerve injury-mediated ED in rat models. In addition, the expression of caspase-3 significantly decreased after treatment with MSCs, suggesting that MSCs might ameliorate ED by decreasing the frequency of apoptotic cells in the corpus cavernosum.

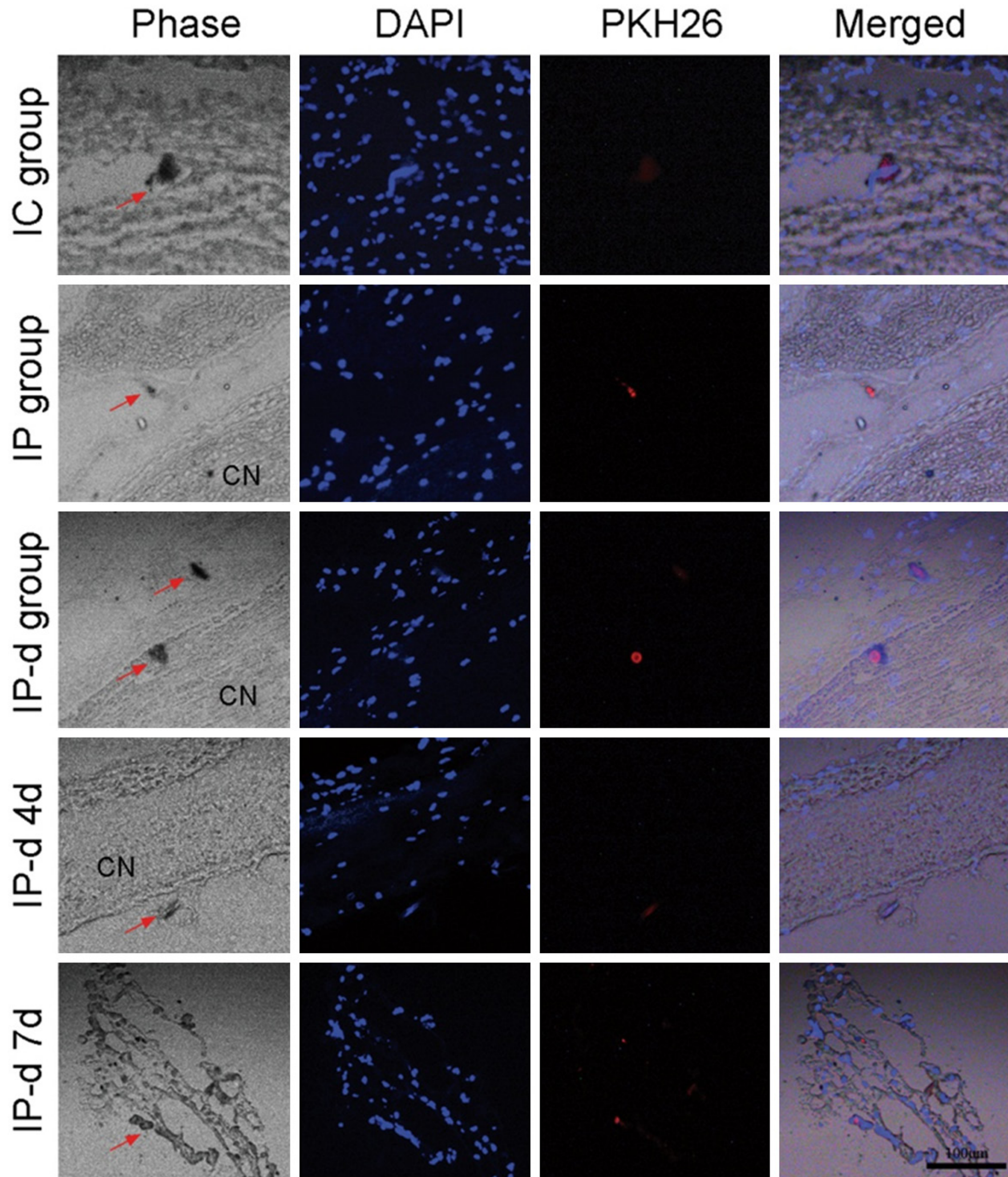

Figure 6. *In vivo* analysis of MSCs survival over time. In the IC group, PKH26 labled MSCs are detectable in the corpus cavernosum. By contrast, in both the IP and IP-d groups, PKH26 labled MSCs are detectable either within or surrounding the CN tissue, but not in the corpus cavernosum. PKH26 labled MSCs are only detectable within the first 2 days after treatment in the IP group, while they are not detectable until 7 days after treatment in the IP-d group. Rats per group: n = 6. Scale bar = 100 μm.

It has been reported that loss of endothelial and smooth muscle contents may result from long-term denervation [24-26]. Therefore, MSCs may help treat ED by differentiating into and replacing lost endothelial cells (ECs) and/or cavernous smooth muscle cells (CSMCs). In the present study, we confirmed that both MSCs and d-MSCs therapy could significantly increase expressions of both PECAM-1 and α-actin in the corpus cavernosum, as well as restore cavernous endothelial and smooth muscle cell populations. Moreover, in a pilot study (data not

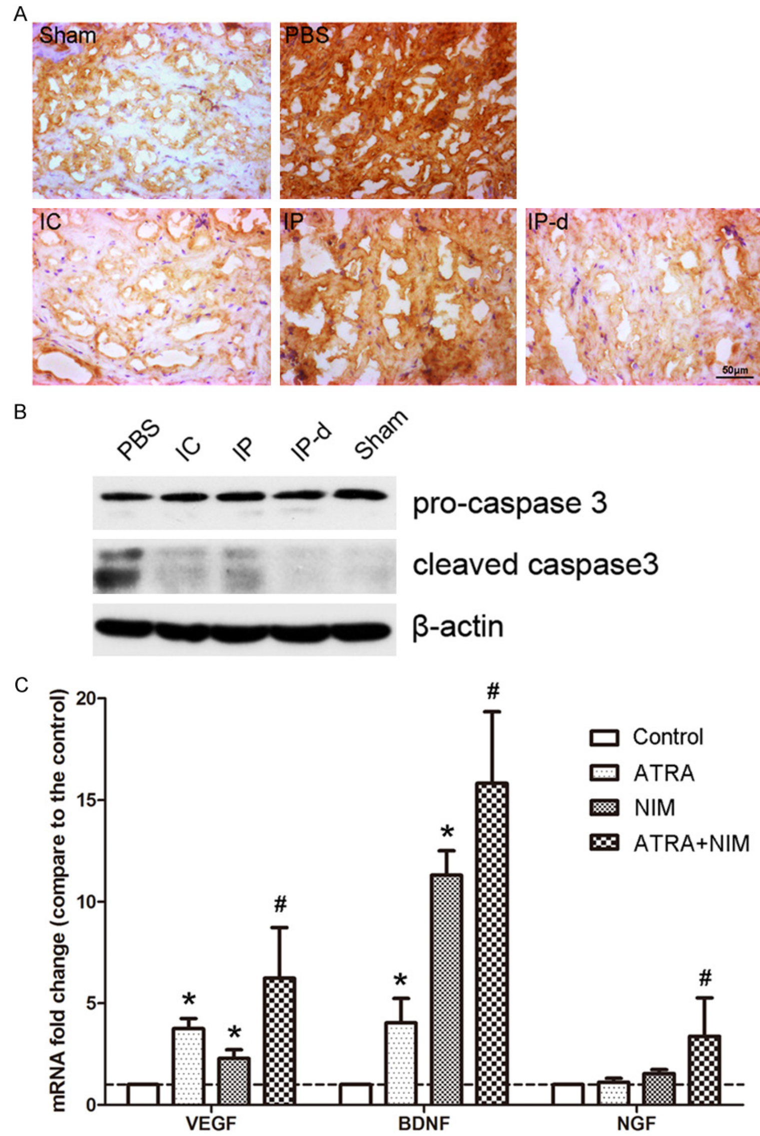

Figure 7. Underlying mechanisms of MSCs-mediated restoration of erectile function. A. Compared to the sham group, the expression of caspase-3 in the corpus cavernous significantly increased in the PBS group, and decreased after treatment with MSCs in the IC and IP-d groups. Rats per group: n = 4. Scale bar = 50 μm. B. Compared to the sham group, the expression of cleaved caspase-3 significantly increased in the PBS group, and decreased after treatment with MSCs in the IC and IP-d groups. Rats per group: n = 4. C. After induction by ATRA and culture in neural induction medium (NIM), d-MSCs exhibited higher expression levels of VEGF, NGF, and BDNF than the MSCs in the group of control, single induced by ATRA or single cultured in NIM. *$P < 0.05$ vs. control group, $^{\#}P < 0.05$ vs. control, ATRA and NIM groups, respectively.

shown), unlike periprostatic implantation, intracavernous injection of neural-differentiated MSCs was not effective in ameliorating erectile function in CNI rats. This result may be explained by the inability of neural-differentiated MSCs to differentiate into endothelial or cavernous smooth muscle cells.

Deficiency of penile nNOS is believed to be related to nerve damage-mediated ED, and may underlie the inefficacy of phosphodiesterase type 5 inhibitors in these patients [27]. In this study, we demonstrated that both MSCs and d-MSCs could enhance nNOS expression and restore erectile function in CNI rats. Thus, MSCs-based therapy may increase the sensitivity of patients with nerve damage-mediated ED to phosphodiesterase type 5 inhibitors.

Intracavernous injection is the most common method of MSCs-based therapy in animal models of ED. Recently, periprostatic implantation of MSCs has also been shown to be effective in CNI animals. Fandel et al [28] found that the therapeutic efficacy of stem cells in CNI models could be attributed to stem cell trafficking to the MPG. Thus, implantation of stem cells near the injured CN or MPG might provide abundant stem cells to the MPG and restore erectile function. Our study demonstrated that periprostatic implantation of MSCs could effectively increase ratios of mICP and tICP to MAP, and ameliorate erectile function in CNI rats. This result may be attributed to trafficking of MSCs to the MPG. From a clinical point of view, compared to intracavernous injection of MSCs, periprostatic MSCs implantation may be a more acceptable method of stem cell therapy. Intracavernous injection of cells or drugs is painful and may cause penile induration. By contrast, periprostatic implantation of MSCs could be performed during pelvic surgery in the event of PAN damage. If necessary, it could also be performed multiple times postoperatively with ultrasound guidance.

In this study, it appeared that IP injection of d-MSCs could better restore erectile function compared to IP injection of primary MSCs. An analysis of *in vivo* MSCs survival over time revealed that d-MSCs exhibited enhanced viability compared to primary MSCs. Moreover, MSCs could increase the frequency of penile nNOS-positive nerve fibers by secreting neurotrophic factors [29], and paracrine signaling by MSCs-derived factors has been shown to play an important role in MSCs therapy [30, 31]. In this study, d-MSCs expressed significantly higher levels of VEGF, NGF and BDNF than primary MSCs. Thus, it is reasonable to postulate that d-MSCs surrounding the prostate might restore cavernous nerve fibers by secreting neurotrophic factors.

In summary, this study shows, for the first time, that periprostatic implantation of neural differentiated MSCs, can effectively ameliorate erectile function in CNI rats. These effects may be ascribed to both decreases in the frequency of apoptotic cells, as well as paracrine effects of d-MSCs-derived factors. Because periprostatic implantation of MSCs is less painful than intracavernous injection, the former approach is more practical for clinical application. Ultimately, delivery of differentiated MSCs may circumvent the risks of injecting primary MSCs with multi-lineage differentiation potentials, and thus accelerate the clinical application of MSCs for the restoration of cavernous nerve function.

Acknowledgements

The study was supported by grants from the Industry-Academia-Research Major Project of the Guangzhou Science and Technology Program (No. 2060404); the Science and Technology Planning Project of Guangdong Province, China (No. 2014A020211009); the Natural Science Foundation of Guangdong Province, China (No. 2015A030313063); the Medical Scientific Research Foundation of Guangdong Province, China (No. A2015318); the China Postdoctoral Science Foundation (No. 2014M560689); and the National Natural Science Foundation of China (No. 81402426).

Disclosure of conflict of interest

None.

Address correspondence to: Hong-Bo Wei, Department of Gastrointestinal Surgery, The Third Affiliated Hospital of Sun Yat-sen University, Tianhe Road 600, Guangzhou 510630, China. Tel: +86-020-85252228, Fax: +86-020-85253336. E-mail: weihbsysu@163.com

References

[1] Hendren SK, O'Connor BI, Liu M, Asano T, Cohen Z, Swallow CJ, Macrae HM, Gryfe R and McLeod RS. Prevalence of male and female sexual dysfunction is high following surgery for rectal cancer. Ann Surg 2005; 242: 212-223.

[2] Sivarajan G, Prabhu V, Taksler GB, Laze J and Lepor H. Ten-year outcomes of sexual function after radical prostatectomy: results of a prospective longitudinal study. Eur Urol 2014; 65: 58-65.

[3] Salonia A, Burnett AL, Graefen M, Hatzimouratidis K, Montorsi F, Mulhall JP and Stief C. Prevention and management of postprostatectomy sexual dysfunctions. Part 1: choosing the right patient at the right time for the right surgery. Eur Urol 2012; 62: 261-272.

[4] Kim NK, Aahn TW, Park JK, Lee KY, Lee WH, Sohn SK and Min JS. Assessment of sexual and voiding function after total mesorectal excision with pelvic autonomic nerve preservation in males with rectal cancer. Dis Colon Rectum 2002; 45: 1178-1185.

[5] Matsumoto T, Ohue M, Sekimoto M, Yamamoto H, Ikeda M and Monden M. Feasibility of autonomic nerve-preserving surgery for advanced rectal cancer based on analysis of micrometastases. Br J Surg 2005; 92: 1444-1448.

[6] Luca F, Valvo M, Ghezzi TL, Zuccaro M, Cenciarelli S, Trovato C, Sonzogni A and Biffi R. Impact of robotic surgery on sexual and urinary functions after fully robotic nerve-sparing total mesorectal excision for rectal cancer. Ann Surg 2013; 257: 672-678.

[7] Shirouzu K, Ogata Y and Araki Y. Oncologic and functional results of total mesorectal excision and autonomic nerve-preserving operation for advanced lower rectal cancer. Dis Colon Rectum 2004; 47: 1442-1447.

[8] Masaki T, Matsuoka H, Kobayashi T, Abe N, Takayama M, Tonari A, Sugiyama M and Atomi Y. Quality assurance of pelvic autonomic nerve-preserving surgery for advanced lower rectal cancer--preliminary results of a randomized controlled trial. Langenbecks Arch Surg 2010; 395: 607-613.

[9] Prockop DJ. Repair of tissues by adult stem/progenitor cells (MSCs): controversies, myths, and changing paradigms. Mol Ther 2009; 17: 939-946.

[10] Sdrimas K and Kourembanas S. MSC microvesicles for the treatment of lung disease: a new paradigm for cell-free therapy. Antioxid Redox Signal 2014; 21: 1905-1915.

[11] Ryu JK, Kim DH, Song KM, Yi T, Suh JK and Song SU. Intracavernous delivery of clonal mesenchymal stem cells restores erectile function in a mouse model of cavernous nerve injury. J Sex Med 2014; 11: 411-423.
[12] You D, Jang MJ, Lee J, Jeong IG, Kim HS, Moon KH, Suh N and Kim CS. Periprostatic implantation of human bone marrow-derived mesenchymal stem cells potentiates recovery of erectile function by intracavernosal injection in a rat model of cavernous nerve injury. Urology 2013; 81: 104-110.
[13] Breitbach M, Bostani T, Roell W, Xia Y, Dewald O, Nygren JM, Fries JW, Tiemann K, Bohlen H, Hescheler J, Welz A, Bloch W, Jacobsen SE and Fleischmann BK. Potential risks of bone marrow cell transplantation into infarcted hearts. Blood 2007; 110: 1362-1369.
[14] Herberts CA, Kwa MS and Hermsen HP. Risk factors in the development of stem cell therapy. J Transl Med 2011; 9: 29.
[15] Guan K, Chang H, Rolletschek A and Wobus AM. Embryonic stem cell-derived neurogenesis. Retinoic acid induction and lineage selection of neuronal cells. Cell Tissue Res 2001; 305: 171-176.
[16] Bi Y, Gong M, Zhang X, Zhang X, Jiang W, Zhang Y, Chen J, Liu Y, He TC and Li T. Pre-activation of retinoid signaling facilitates neuronal differentiation of mesenchymal stem cells. Dev Growth Differ 2010; 52: 419-431.
[17] Liu Y, Zhang X, Dai Y, Shu C, Qu P, Liu YX, Yang L and Li TY. [Effects of bone marrow mesenchymal stem cells on learning and memory functional recovery in neonatal rats with hypoxic-ischemic brain damage]. Zhonghua Er Ke Za Zhi 2008; 46: 648-653.
[18] Woodbury D, Schwarz EJ, Prockop DJ and Black IB. Adult rat and human bone marrow stromal cells differentiate into neurons. J Neurosci Res 2000; 61: 364-370.
[19] Jin HR, Chung YG, Kim WJ, Zhang LW, Piao S, Tuvshintur B, Yin GN, Shin SH, Tumurbaatar M, Han JY, Ryu JK and Suh JK. A mouse model of cavernous nerve injury-induced erectile dysfunction: functional and morphological characterization of the corpus cavernosum. J Sex Med 2010; 7: 3351-3364.
[20] Dorsey P, Keel C, Klavens M and Hellstrom WJ. Phosphodiesterase type 5 (PDE5) inhibitors for the treatment of erectile dysfunction. Expert Opin Pharmacother 2010; 11: 1109-1122.
[21] Albersen M, Kendirci M, Van der Aa F, Hellstrom WJ, Lue TF and Spees JL. Multipotent stromal cell therapy for cavernous nerve injury-induced erectile dysfunction. J Sex Med 2012; 9: 385-403.
[22] Lin CS, Xin ZC, Wang Z, Deng C, Huang YC, Lin G and Lue TF. Stem cell therapy for erectile dysfunction: a critical review. Stem Cells Dev 2012; 21: 343-351.
[23] Qiu X, Lin H, Wang Y, Yu W, Chen Y, Wang R and Dai Y. Intracavernous transplantation of bone marrow-derived mesenchymal stem cells restores erectile function of streptozocin-induced diabetic rats. J Sex Med 2011; 8: 427-436.
[24] Iacono F, Giannella R, Somma P, Manno G, Fusco F and Mirone V. Histological alterations in cavernous tissue after radical prostatectomy. J Urol 2005; 173: 1673-1676.
[25] Leungwattanakij S, Bivalacqua TJ, Usta MF, Yang DY, Hyun JS, Champion HC, Abdel-Mageed AB and Hellstrom WJ. Cavernous neurotomy causes hypoxia and fibrosis in rat corpus cavernosum. J Androl 2003; 24: 239-245.
[26] User HM, Hairston JH, Zelner DJ, McKenna KE and McVary KT. Penile weight and cell subtype specific changes in a post-radical prostatectomy model of erectile dysfunction. J Urol 2003; 169: 1175-1179.
[27] Zagaja GP, Mhoon DA, Aikens JE and Brendler CB. Sildenafil in the treatment of erectile dysfunction after radical prostatectomy. Urology 2000; 56: 631-634.
[28] Fandel TM, Albersen M, Lin G, Qiu X, Ning H, Banie L, Lue TF and Lin CS. Recruitment of intracavernously injected adipose-derived stem cells to the major pelvic ganglion improves erectile function in a rat model of cavernous nerve injury. Eur Urol 2012; 61: 201-210.
[29] Sun C, Lin H, Yu W, Li X, Chen Y, Qiu X, Wang R and Dai Y. Neurotrophic effect of bone marrow mesenchymal stem cells for erectile dysfunction in diabetic rats. Int J Androl 2012; 35: 601-607.
[30] Gnecchi M, Zhang Z, Ni A and Dzau VJ. Paracrine mechanisms in adult stem cell signaling and therapy. Circ Res 2008; 103: 1204-1219.
[31] Prockop DJ. "Stemness" does not explain the repair of many tissues by mesenchymal stem/multipotent stromal cells (MSCs). Clin Pharmacol Ther 2007; 82: 241-243.